

DYNAMICAL COMPETITION BETWEEN REACTIVE AND REACTIVE DETACHMENT CHANNELS IN $X^- + H_2$ COLLIDING SYSTEMS ($X = Cl, Br, I$)

M. DURUP-FERGUSON

LPCR Université Paris-Sud, 91405 Orsay, France

J.C. BRENOT, J.A. FAYETON, K. PROVOST and M. BARAT

LCAM Université Paris-Sud, 91405 Orsay, France

Received 11 February 1987

Two reactive processes are observed: $X^- + H_2 \rightarrow XH + H^-$ (R) and $X^- + H_2 \rightarrow XH + H + e^-$ (RD). The angular and energy distributions of the molecular XH products are measured at collision energies varying from 5 to 10 eV center of mass. These distributions obey identical rules in the three systems: (a) XH molecules formed by both R and RD processes are scattered at the same c.m. angle, respectively $55^\circ \pm 10$ for ClH, $80^\circ \pm 20$ for BrH and $90^\circ \pm 20$ for IH. (b) The rovibrational energy of the XH molecules, when formed by R processes, is limited to a small amount: ≤ 2 eV for ClH, ≤ 1.5 eV for BrH, ≤ 1 eV for IH, whereas when formed by RD it extends to the highest amount available from the collision energy, up to the dissociation limit. The RD process is not observed experimentally in the I^-/H_2 system. This dynamical behaviour is fully understood in terms of non-adiabatic interaction between the two lowest $[XH_2]^-$ ionic surfaces, but the reason of the angular anisotropy is still not well understood.

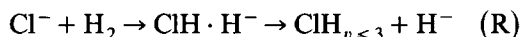
1. Introduction

A multiconcident analysis of two products of the collisional $Cl^- + H_2$ system has been previously described [1]. Energy and angular distributions of the two families of HCl molecules formed by reactive (R) ($HCl + H^-$) and reactive detachment (RD) ($HCl + H + e^-$) processes, respectively, were independently obtained. These distributions have remarkable features, some of which are explained by the topology of the two lowest adiabatic surfaces of the $[ClH_2]^-$ system as they appear in the asymptotic product cut.

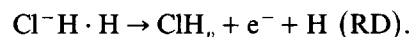
The competition between R and RD channels depends on the interaction between the two lowest surfaces along the avoided crossing seam (fig. 1). The apex at infinite XH–H distance of their conical intersection is a real crossing in the asymptotic product cut due to the existence of the ground state of HCl^- which is stable at large internuclear distance but vanishes at shorter distances into the detachment continuum.

The competition is seen as an electron transfer

within the $[ClH_2]^-$ pseudomolecule:



↓



In order to check this mechanism, the analogous systems Br^-H_2 and I^-H_2 have been investigated. The same qualitative features of the angular and energy distributions of the XH molecules are observed. The quantitative differences confirm the critical role of the HX^- intermediate ion.

Recent theoretical calculations performed by Sizun et al. [2] confirm the relevance of this basic idea and have led to a deeper understanding of the dynamics involved on such $[H_2X]^-$ surfaces.

2. Experimental

The experimental arrangement has been described in detail previously [1,3]. A beam of fast

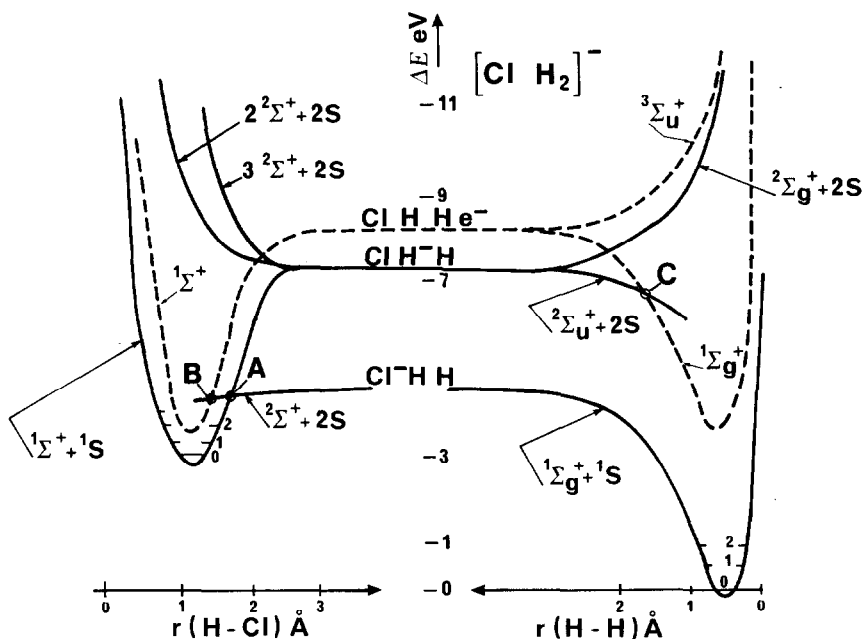


Fig. 1. Energy diagram of $[\text{H}_2\text{Cl}]^-$ system in two asymptotic cuts: right-hand side entrance partners, left-hand side exit products.

ions crosses a supersonic beam of H_2 molecules at right angles. The scattered fast neutral species (X , XH) and the negative ones (e^- , H^-) are coincidentally detected on two independent position-sensitive detectors using microchannel plates with resistive collectors. The time delays of the two types of products and their impinging positions on their respective collectors can be correlated. The neutral detector is perpendicular to the X^- beam; the electrons and H^- ions are extracted from the collision region by a transverse electric field towards a collector parallel to the $\text{X}^- \cdot \text{H}_2$ plane (fig. 2). The extracting field introduces a dissym-

metry in the geometry of the apparatus: the impinging positions of the H^- depend on its strength. In these experiments the corresponding information has not been used. The $N(\Delta t, X, Y)$ spectra correspond to the delay time spectra of neutrals detected in each pixel of the front detector and their correlated electrons or H^- .

The raw data consist in intensity (I) plots as a function of delay time (Δt) for various scattering laboratory angles θ . For peaks corresponding to an electron coincidence, this $I(\theta, \Delta t)$ is directly transformed into $I(v, \chi)$ where v and χ are respectively the velocity and the scattering angle of the neutral product with respect to the original direction of the projectile ion beam in the center of mass frame. For peaks corresponding to H^- coincidence this transformation goes through a simulation program [1].

In this paper only the results corresponding to the two reactive channels are reported: the other peaks which were experimentally observed, namely the simple detachment (SD) and the dissociative detachment (DD) processes, have been omitted. The data are displayed in the form of contour maps of constant intensity $I(v, \chi)$ of XH in a

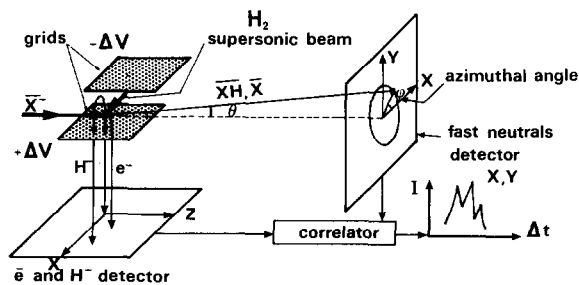


Fig. 2. Schematic diagram of the apparatus.

polar coordinate system in which the radial coordinate represents the speed of the product XH relative to the center of mass and the angular coordinate χ is measured with respect to the original direction of the projectile ion beam. Small values of the radial coordinate correspond to small values of the final relative translational energy of the products and therefore, by energy conservation, to large internal excitation of the product. The various circles correspond to various endothermicities. They are the same for R and RD processes because the kinetic energy of the electron released in RD has been measured to be negligible, therefore for both R and RD the total endothermicity is $Q = \Delta H_{\text{threshold}} + E_{\text{rv}}(\text{XH})$ where E_{rv} is the rovibrational energy.

The angular aperture of the primary ion beam and the size of the pixel determine the angular resolution of the scattered particle. To this laboratory acceptance spread $\Delta\theta$ correspond, in the center-of-mass frame, angular and energy inaccuracies $\Delta\chi$ and ΔQ which, due to our heavy on light-light (HLL) mass combination, increase with

the mass of the projectile:

$$\Delta\chi = \Delta\theta \left\{ 1 + \alpha \cos \chi \left[E_{\text{c.m.}} / (E_{\text{c.m.}} - Q) \right]^{1/2} \right\}, \quad (1)$$

$$\Delta E_{\text{rv}} = \Delta Q = \Delta\theta \left\{ -2Q\alpha \left[E_{\text{c.m.}} / (E_{\text{c.m.}} - Q) \right] \right\}, \quad (2)$$

with

$$\alpha = [A(A+B)/C(B+C)]^{1/2},$$

where $E_{\text{c.m.}}$ is the center-of-mass collision energy, Q the endothermicity of the reaction, A the mass of the projectile and BC the mass of the target molecule. The mass of H_2 being very small compared to the mass of Cl, Br and I projectile α equals its limit value $2^{-1/2}A$.

3. Results

Figs. 3–5 show the contour maps of respectively ClH, BrH and IH formation at two different

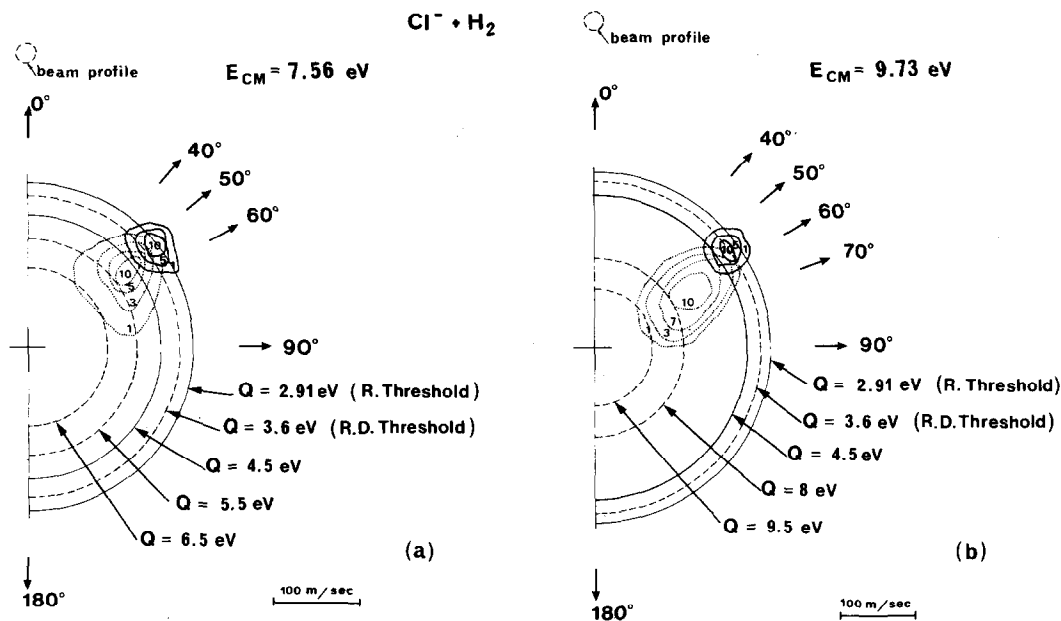


Fig. 3. Contour map of the specific intensity of HCl. The circles labelled $Q = 2.91$ eV and $Q = 4.5$ eV are the locus of threshold energy and highest internal energy observed for HCl formed by R process, respectively. The circle labelled $R = 3.6$ eV is the locus of threshold energy of HCl formed by RD process.

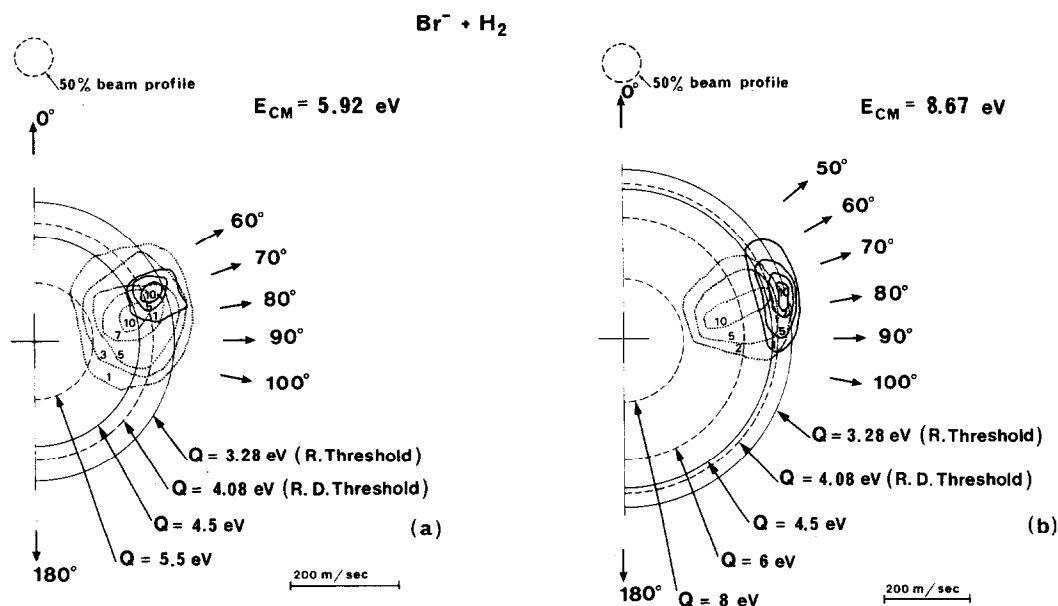


Fig. 4. Contour map of specific intensity of HBr. The circles labelled $Q = 3.28$ eV and $Q = 4.5$ eV are respectively the locus of threshold energy and highest internal energy observed for HBr formed by R processes. The circle labelled $Q = 4.08$ eV is the locus of threshold energy of HBr formed by RD process.

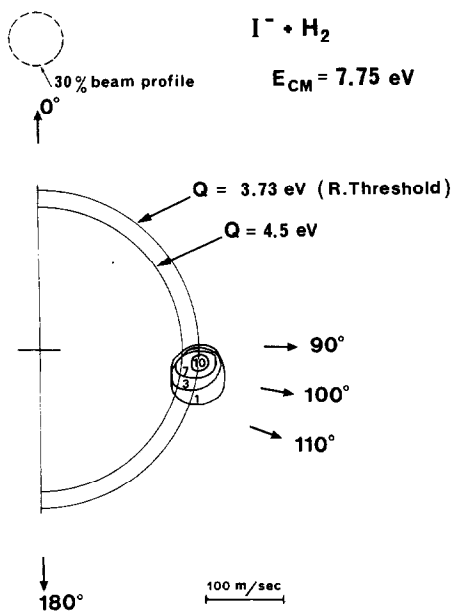


Fig. 5. Contour map of specific intensity of HI. The circles labelled $Q = 3.73$ eV and $Q = 4.5$ eV are respectively the locus of threshold energy and highest internal energy observed for HI formed by R.

collision energies. ClH and BrH are formed by both R and RD processes; the RD process is not experimentally observed in IH formation. As a first remark it is clear that the two processes, when they are both present, could not be separated without the coincidence technique. The three systems exhibit common features belonging mainly to two independent classes, namely:

- *The angular anisotropy of HX production.* The angular distribution of XH is peaked around the same c.m. scattering angle, for both R and RD processes, whatever the collision energy, but dependent on the halogen ion: $\chi = 55^\circ \pm 10$ for HCl, $80^\circ \pm 20$ for BrH and $90^\circ \pm 20$ for HI. The reason of the increasing width of the $I(\chi)$ distribution from Cl to Br to I is purely experimental as seen in eq. (1).

The relative cross sections for RD and SD channels are plotted in fig. 6 as a function of χ for various internal rovibrational excitation energies of respectively XH and H_2 molecules. It is clear that the χ value characteristic of the RD channel corresponds to the limiting value of χ for the SD channel.

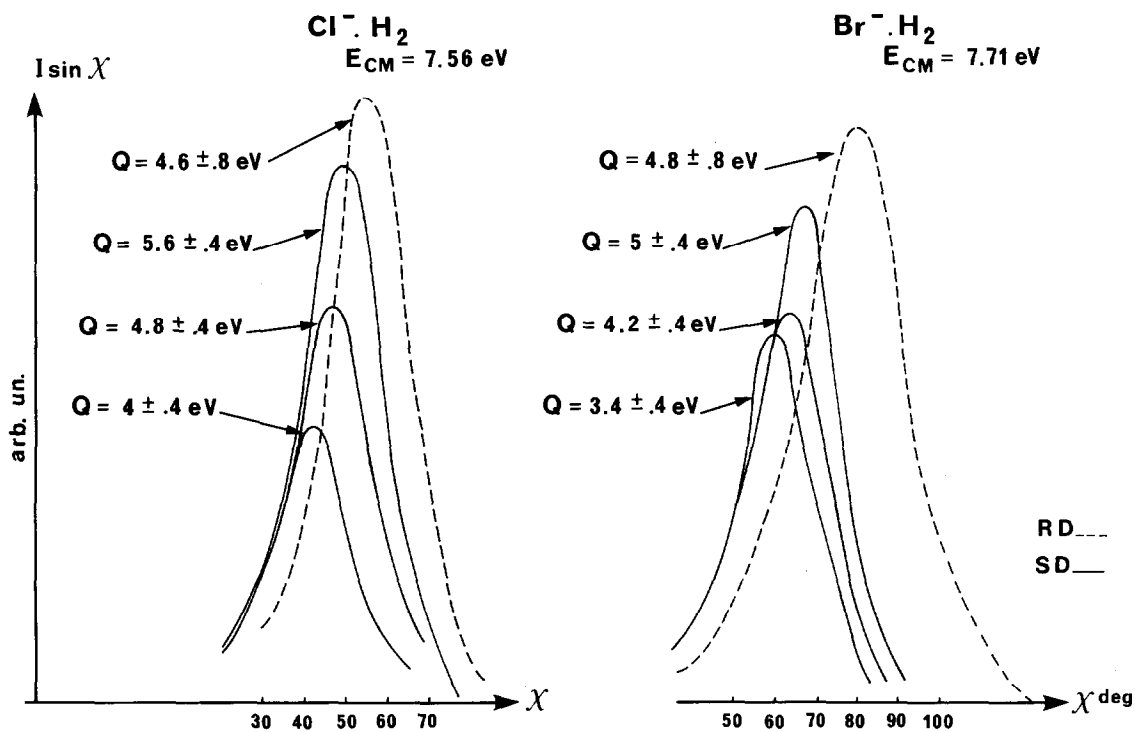


Fig. 6. Angular distributions for RD and SD channels. The angular deflection of HCl and HBr is independent of their internal energy, the angular deflection of Cl and Br increases with internal energy of H₂.

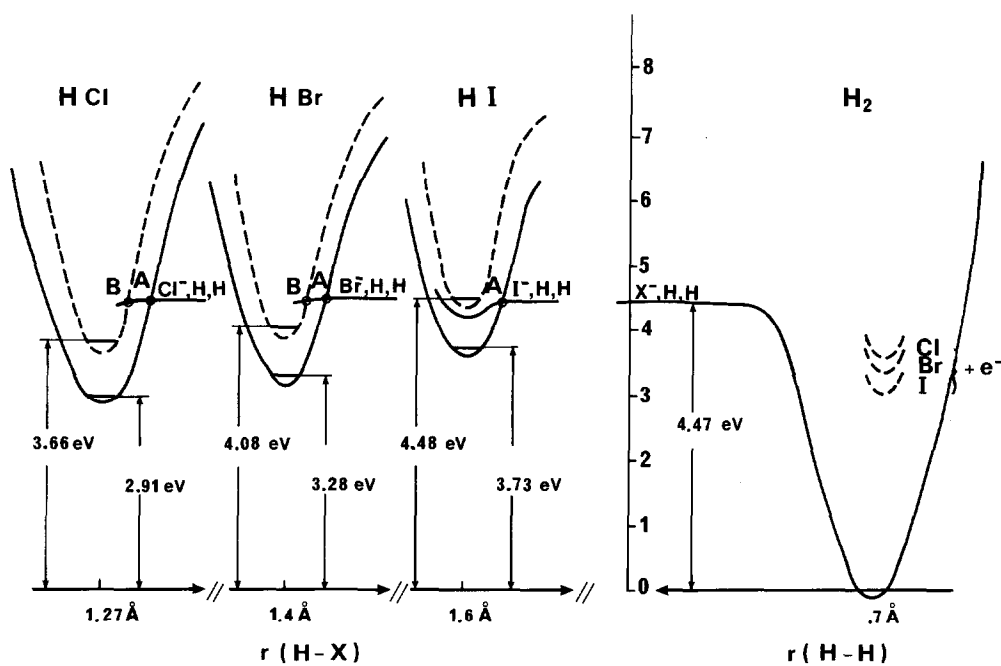


Fig. 7. Energy diagram of the reactive exit channel of the (ClH₂)⁻, (BrH₂)⁻ and (IH₂)⁻ systems pointing out the relative positions of A and B crossings.

– The small rovibrational energy E_{rv} of XH formed by the R processes. $E_{rv}(\text{HCl}) = 1.5 \pm 0.3$ eV, $E_{rv}(\text{HBr}) = 1 \pm 0.5$ eV, $E_{rv}(\text{HI}) = 0.7 \pm 0.5$ eV – contrasting with the fact that for the RD channels, the rovibrational excitation occurs up to the dissociation limit. The equiprobability of excitation of all the levels of excitation of ClH and BrH by RD is shown in figs. 3 and 4.

4. Discussion

The implications of these two remarkable features can be discussed in two different frames.

4.1. The angular distribution and mechanistic model

The independence with collision energy of the χ peaking of the XH product suggests that the reactive path obeys a mechanistic model, independent of details in the shape of potential energy surface.

In refs. [1,3] we discussed the relevance of a sequential impulse model for the HCl formation.

Various impulse models [4,5] in which the atoms interact via hard-sphere potentials have been applied to many direct thermoneutral reactions involving one atom exchange. These models reproduce well the main features of angular and energy distributions of the product for high-energy collisions for which the whole system does not rotate nor vibrate too much during the collision.

In the present case, however, the reaction is endothermic, the collision time is of the order of a vibrational period, and furthermore, two particles, namely an H atom and an electron, are exchanged in opposite directions.

However, Bates' [4] model gave a satisfactory approximation for HCl formation. This model requires an orientation at 45° of the H_2 molecule with respect to the incident beam. The whole collisional process is then seen as two successive binary collisions in which X hits the first H impulsively and then this H atom hits in turn the other H in a like manner. The Cl combines with one of the two Hs if their relative energy is less than the dissociation energy. The calculated scattering angle in the limit of infinite mass of X is found to be

45° [1]. However, the experimental χ value increases from Cl, Br to I instead of converging to 45° .

Such successive collisions of the central hydrogen atom as invoked in the impulse model have been shown to occur in HLL mass combination systems by theoretical surface trajectory calculations [6]. In such systems the potential energy surface representing the collinear approach is strongly skewed which causes the system to cut the corner by successive rebounds on the two repulsive walls. Such trajectories produce sharp oscillations in the LL bond length when the new bond is formed. In other words the central light atom trapped between a heavy and a light atom undergoes multiples collisions on these two partners in the process of formation of the new HL bond.

Sizun et al. [2] have well reproduced the χ peaking of the R process by surface hopping calculations on the two lowest diabatic surfaces (calculated by the DIM procedure) of the $\text{Cl}^- \text{H}_2$ system at 9.7 eV center-of-mass collision energy. These authors also have checked the independence of their differential cross section with the coupling between the two diabatic ionic surfaces and the relative position of the neutral one. They thought that this result is consistent with the sequential impulse model which is insensitive to details of the PES. However, they did not check the influence of the position of the crossing seam of the two diabatic surfaces. In order to gain more insight into the mechanism these authors have also determined the probability of producing each channel as a function of the impact parameter and of the angle of attack β at the crossing seam (β is the angle between H_2 molecule axis and the vector drawn from Cl to the c.m. of the H_2 molecule). The angle of attack of 45° is found to favor the R process and the favorable impact parameter decreases from SD to R to RD. This last finding is in agreement with our experimental result shown in fig. 6. The larger are the excitation of H_2 and the deflection χ angle of Cl in the SD channel, the shorter is the impact parameter down to a limit at which the SD process disappears while the RD is enhanced.

It is perhaps worthwhile to compare with the slightly endothermic parent neutral reaction $\text{Cl} +$

$\text{H}_2 \rightarrow \text{HCl} + \text{H}$, for which some experimental scattering results are available. They indicate that the product is mainly back scattered [7]. Classical trajectory calculations on a LEPS surface reproduce that result [8]. From the trajectory calculations performed at various collision energies, Persky concludes that the scattering angle is mainly dependent on the impact parameter: when the impact parameter increases the scattering angle shifts to lower angles.

This latter fact may be an indication that in the X^-H_2 systems, in contrast to the XH_2 systems, the reactive processes would occur at a fixed impact parameter independent of the collision energy, at a value depending on the radius of the orbiting p electron.

However, it is still impossible to conclude whether the angular anisotropy of the HX molecule is due to a typical topology of the potential energy surface of such systems or to a purely kinematic type of trajectory independently of the surfaces.

The analysis of the F^-/H_2 system will perhaps shed some light on this problem.

4.2. Rovibrational energy distribution and surface crossing

The similitude of the dynamical behaviour of the three systems leads to an extension of the discussion which has been given for the $[\text{ClH}_2]^-$ system.

In that discussion a simple understanding of the competition between the two reactive channels was obtained by just considering the asymptotic potential curves corresponding to non-interacting particles. In figs. 1 and 7 are presented the asymptotic cut, on the right-hand side in the incident channel at infinite $\text{X}-\text{H}_2$ distance and at the left-hand side in the reactive product channels at infinite $\text{XH}-\text{H}$ distance. On that side are drawn the energy curves of HX formed with H^- and in the detachment continuum (dashed curve). The $[\text{XH}_2]^-$ representation has to take into account the X^-H states. The ground $2^2\Sigma^+$ state dissociates in $\text{X}^- + \text{H}$ and cuts the XH curve in point A. In $[\text{ClH}_2]^-$ [9] and $[\text{BrH}_2]^-$ [10] this state disappears into the continuum at shorter XH distance. By contrast the ground state of HI^- is attractive

and stable with respect to electron detachment over a large range of internuclear distances [11]. These systems exhibit clearly two $[\text{XH}_2]^-$ surfaces and a neutral one. Point A can be seen as the apex of an avoided crossing between the two lowest adiabatic surfaces of the $[\text{XH}_2]^-$ systems. The lowest one leads to $\text{HX} + \text{H}^-$ and dissociates into $\text{X}^- + \text{H} + \text{H}$, the upper one leads to $\text{HX}^- + \text{H}$ which autodetaches giving $\text{XH} + \text{e}^- + \text{H}$ and dissociates into $\text{X} + \text{H} + \text{H}^-$. Point A can also be seen as the apex of the crossing seam of the two diabatic surfaces, one corresponding to $\text{Cl}^- + \text{H}_2$ in the reactant region and $\text{HX}^- + \text{H}$ in the product region. This surface leads to the RD process when X^-H penetrates in the detachment continuum. The other diabatic surface corresponds to $\text{HX} + \text{H}^-$ in the product region and is correlated in the reactant region to $\text{X} + \text{H}_2^-$ which leads to non-reactive detachment process (SD).

It is clear from the DIM surfaces calculated by Sizun et al. [2] that no product channels are accessible if the trajectory does not reach the ionic crossing. At the point A the interaction between the two surfaces is zero, but at shorter internuclear distances the seam is the locus of a strong $\text{XH} \cdot \text{H}^- \rightleftharpoons \text{X}^-\text{H} \cdot \text{H}$ electron exchange interaction. The limiting value of XH rovibrational excitation energy in the $\text{XH} + \text{H}^-$ channel is that for which the probability of the electron transfer to $\text{X}^-\text{H} \cdot \text{H}$ is maximum. An upper limit is given by the position of A, figs. 1 and 8. The A crossing lies at or slightly below the energy of the $\text{X}^- + \text{H}$ asymptote which is in the energy scale of the $[\text{XH}_2]^-$ systems at the same common value of 4.49 eV (H_2 bond energy). The calculated maximum values of internal energy of XH are respectively 1.8 eV for HCl, 1 eV for HBr and 0.7 eV for HI, in excellent agreement with the experimental data. At smaller $\text{H}-\text{X}$ enters the continuum of HCl and HBr at the B crossing giving rise to $\text{HX} + \text{e}^- + \text{H}$. In the I^-/H_2 system, the potential curve is attractive and stable with respect to electron autodetachment over a large range of internuclear distances [11] precluding any electron detachment. This explains why reactive detachment is not observed experimentally in this system. In that case the HI^- formation is followed by dissociation into $\text{I}^- + \text{H}$, a channel that cannot be observed in our experiment.

Therefore it is now clear that the dynamics of the (halogen)⁻H₂ reactions are dominated by the interaction between the two lowest ionic surfaces, the location of their seam and the relative position of the neutral surfaces.

It is also clear that the reaction R which belongs to the family of reactions X⁻ + HY → XH + Y⁻, usually considered as proton transfer [12] reactions, is not a one-step reaction in which the negative ion is the acceptor of a proton from a neutral molecule. It is a more complex reaction involving an H transfer plus an electron transfer in the opposite sense X⁻⋯HH. The experimental data are well explained by a mechanism involving H stripping as a first step leading to Cl⁻H·H, followed by the electron transfer as the second step. The energy barrier for the R process would be given by the level of the seam; this is not incompatible with the experimental measurements of Huq et al. [13] who observed the R process at the very threshold, the Cl⁻-H₂ diabatic surfaces calculated by Sizun et al. [2] show clearly that at short internuclear distances the seam is at an energy level equal to the endothermic threshold of R reaction.

The rate constant of the reverse exothermal reaction has been recently measured at thermal energy in a flow tube experiment [14] for H⁻ + HCl → Cl⁻ + H₂. This rate constant is equal to half the Langevin orbiting rate constant, which means that half the collisions are efficient. The fact that the cross section of Cl⁻ + H₂ → HCl + H⁻ is very low [13] when the endothermicity is overcome by kinetic energy indicates from a “detailed balance” argument that the exothermicity of the reverse reaction does not result in relative kinetic energy of the Cl⁻ and H₂ products but in rovibrational energy of the H₂ molecule. In return, this means that a rovibrational excitation of H₂ would lead to a cross section higher by many orders of magnitude for the direct reaction. Unfortunately, this cannot be checked in our experiment. An increase in the cross section for the neutral reactions [15,16] X + H₂ → XH + H is also observed when the endothermicity of the reaction is supplied by vibrational excitation of H₂ instead of relative kinetic energy of the reactants. This is a usual behaviour for many endothermic reactions

and many classical trajectory calculations have shown the importance of the location of the barrier and other features of the potential energy surface [17–19].

In the X⁻ + H₂ system not only the position of the endothermic barrier but the shape and the location of the region of strong non-adiabatic interaction are the features which can have major effects on the dynamics of the reactive collision. Moreover in this particular HLL mass combination recrossing or multiple crossing of the seam can occur [20].

5. Conclusion

The competition between the two reactive channels R and RD of the X⁻-H₂ collisional systems is clearly dominated by the non-adiabatic interaction between the two lowest ionic potential surfaces. On the other hand, the parameters determining the anisotropy of the angular distribution of the XH product are still an open question.

Acknowledgement

The authors have enjoyed useful discussions with V. Esaulov, J.P. Gauyacq, E. Gislason, V. Sidis and M. Sizun.

References

- [1] M. Barat, J.C. Brenot, J.A. Fayeton, J.C. Houver, J.B. Ozenne, R.S. Berry and M. Durup-Ferguson, *Chem. Phys.* 97 (1985) 165.
- [2] M. Sizun, E.A. Gislason and G. Parlant, *Chem. Phys.* 107 (1986) 327.
- [3] M. Barat, J.C. Brenot, M. Durup-Ferguson, J.A. Fayeton, E. Gislason, J.C. Houver, J.B. Ozenne, G. Parlant and M. Sizun, *Proc. Conf. Recent Advances in Molecular reaction Dynamics, Aussois* (1985).
- [4] D.R. Bates, C.J. Cooks and F.J. Smith, *Proc. Phys. Soc. (London)* 83 (1964) 49.
- [5] J.C. Light and J. Horrocks, *Proc. Phys. Soc. (London)* 84 (1964) 527;
R.J. Suplinskas, *J. Chem. Phys.* 49 (1968) 5046;
P.J. Kuntz, *Trans. Faraday Soc.* 66 (1970) 2980;
R. Grice and D.R. Hardin, *Mol. Phys.* 21 (1971) 805;
H.T. Marron, *J. Chem. Phys.* 58 (1973) 153;

- B.H. Mahan, W.E.W. Ruska and J.S. Winn, *J. Chem. Phys.* 65 (1976) 3888.
- [6] J.C. Polanyi and J.L. Schreiber, *Discussions Faraday Soc.* 62 (1977) 267;
C.A. Parr, J.C. Polanyi and W.H. Wong, *J. Chem. Phys.* 58 (1973) 5.
- [7] J.D. McDonald, Doctoral thesis, Harvard University, USA (1970).
- [8] A. Persky, *J. Chem. Phys.* 66 (1977) 2932.
- [9] R. Azria, Y. le Coat, D. Simon and M. Tronc, *J. Phys. B* 13 (1980) 1909;
D. Teillet-Billy and J.P. Gauyacq, *J. Phys. B* 17 (1984) 4041;
S.V. O'Neill, P. Rosmus, D.W. Norcross and H.J. Werner, *J. Chem. Phys.* 85 (1986) 7232.
- [10] R. Abouaf and D. Teillet Billy, *Chem. Phys. Letters* 73 (1980) 106.
- [11] D. Spence, W.A. Chupka and C.M. Stevens, *J. Chem. Phys.* 76 (1982) 2759.
- [12] D.K. Bohme, in: *Interactions between ions and molecules*, ed. P. Ausloos (Plenum Press, New York, 1975) pp. 489 ff.
- [13] M. Huq, D.S. Fraedrich, L. Doverspike, R.L. Champion and V.A. Esaulov, *J. Chem. Phys.* 76 (1982) 4953.
- [14] I. Dotan, M. Durup-Ferguson and J. Filley, unpublished results.
- [15] D.H. Stedman, D. Steffenson and H. Niki, *Chem. Phys. Letters* 7 (1970) 173.
- [16] L.B. Sims, L.R. Dossier and P.S. Wilson, *Chem. Phys. Letters* 32 (1975) 150.
- [17] D.S. Perry, J.C. Polanyi and C.W. Wilson, *Chem. Phys.* 3 (1974) 317.
- [18] J.W. Duff and D.G. Truhlar, *J. Chem. Phys.* 62 (1975) 2744.
- [19] D.S. Perry, J.C. Polanyi and C.W. Wilson, *Chem. Phys. Letters* 24 (1974) 484.
- [20] H.R. Mayne, J.C. Polanyi and J.C. Tully, *J. Chem. Phys.* 82 (1985) 161.